

# **Report ITU-R S.2565-0**

## **(11/2025)**

S Series: Fixed-satellite service

**Simulation results of fuselage  
attenuation for Aeronautical Earth  
Stations In Motion (A-ESIM) in the  
27.5-29.5 GHz band**



## Foreword

The role of the Radiocommunication Sector is to ensure the rational, equitable, efficient and economical use of the radio-frequency spectrum by all radiocommunication services, including satellite services, and carry out studies without limit of frequency range on the basis of which Recommendations are adopted.

The regulatory and policy functions of the Radiocommunication Sector are performed by World and Regional Radiocommunication Conferences and Radiocommunication Assemblies supported by Study Groups.

## Policy on Intellectual Property Right (IPR)

ITU-R policy on IPR is described in the Common Patent Policy for ITU-T/ITU-R/ISO/IEC referenced in Resolution ITU-R 1. Forms to be used for the submission of patent statements and licensing declarations by patent holders are available from <https://www.itu.int/ITU-R/go/patents/en> where the Guidelines for Implementation of the Common Patent Policy for ITU-T/ITU-R/ISO/IEC and the ITU-R patent information database can also be found.

### Series of ITU-R Reports

(Also available online at <https://www.itu.int/publ/R-REP/en>)

Series	Title
<b>BO</b>	Satellite delivery
<b>BR</b>	Recording for production, archival and play-out; film for television
<b>BS</b>	Broadcasting service (sound)
<b>BT</b>	Broadcasting service (television)
<b>F</b>	Fixed service
<b>M</b>	Mobile, radiodetermination, amateur and related satellite services
<b>P</b>	Radiowave propagation
<b>RA</b>	Radio astronomy
<b>RS</b>	Remote sensing systems
<b>S</b>	<b>Fixed-satellite service</b>
<b>SA</b>	Space applications and meteorology
<b>SF</b>	Frequency sharing and coordination between fixed-satellite and fixed service systems
<b>SM</b>	Spectrum management
<b>TF</b>	Time signals and frequency standards emissions

*Note: This ITU-R Report was approved in English by the Study Group under the procedure detailed in Resolution ITU-R 1.*

Electronic Publication  
Geneva, 2026

© ITU 2026

All rights reserved. No part of this publication may be reproduced, by any means whatsoever, without written permission of ITU.

## REPORT ITU-R S.2565-0

**Simulation results of fuselage attenuation for Aeronautical Earth Stations In Motion (A-ESIM) in the 27.5-29.5 GHz band**

(2025)

**Keywords**

A-ESIM, ESIM, Fuselage attenuation

**Glossary/Abbreviations**

AUT Antenna under test

A-ESIM Aeronautical earth station in motion

ESIM Earth station in motion

MLFMM Multi-level fast multipole method

MOM Method of moments

**Relevant ITU-R Reports**

Report ITU-R M.2221 – Feasibility of MSS operations in certain frequency bands

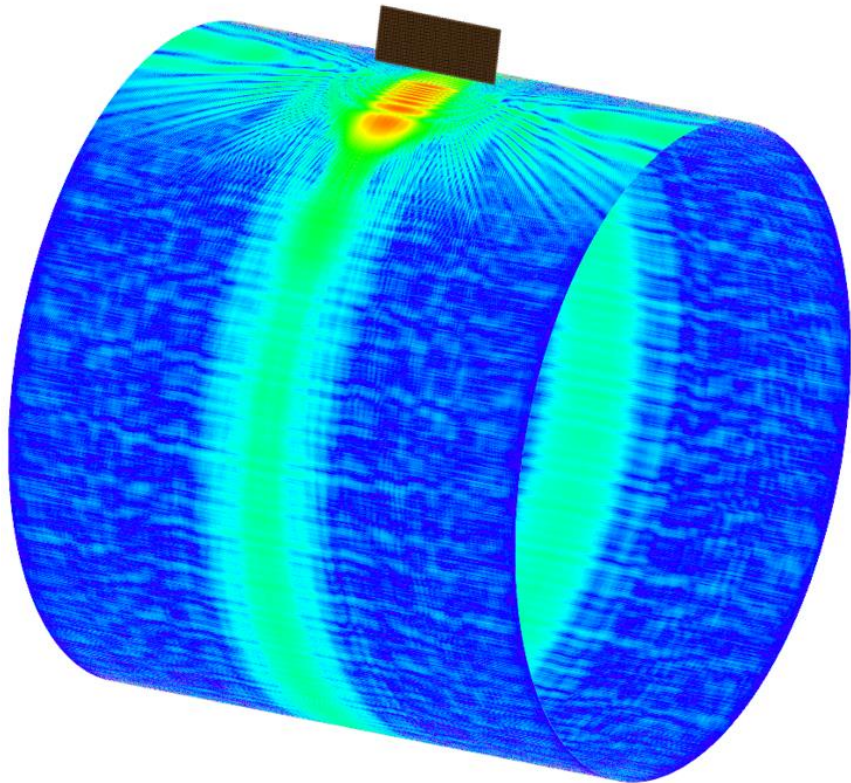
**1 Introduction**

This Report provides simulation results for fuselage attenuation of A-ESIM mounted on two cylindrical simulations of commercial aircrafts in the frequency range 27.5-29.5 GHz. The simulation modelling was simplified to make it more tractable and feasible. The entire aircraft was not modelled, nor the actual shape of the aircraft. A small section of perfectly round cylindrical section was used to model the area right around the ESIM antenna and the creeping wave effects.

**2 Background**

Consideration of fuselage attenuation is important as this attenuation reduces emissions from the ESIM mounted on aircraft toward terrestrial stations on the Earth's surface. An evaluation of fuselage attenuation characteristics is necessary because there may be a possibility of radio frequency (RF) energy radiated below the line-of-sight of the antenna due to "creeping waves" around the fuselage of the aircraft (with an example depicted in Fig. 1). This type of analysis was previously conducted in Report ITU-R M.2221 under § 3.6.2.6.2 "Interference from aircraft earth stations to radio astronomy stations", specifically in Fig. 3.6-14, which proposes an off-axis attenuation (or relative sidelobe envelope loss to the free-space antenna sidelobes) due to the fuselage blockage for an antenna mounted on the fuselage looking port (left) and starboard (right) on the narrow side of the fuselage or azimuth 90 degrees at Ku-band (14.2 GHz) based on antenna measurements. While the instant analysis is based on cylindrical simulations, the analysis in Report ITU-R M.2221 was based on "a measurement campaign run by an aeronautical Internet Service Provider has been considered as reference. In this particular study, the attenuation due to the aircraft body on the roll-plane (i.e. for azimuth = 90°) has been measured when an antenna was mounted on top of a full cylinder with radius of curvature approximately equal to that of a Boeing 737 fuselage."

FIGURE 1  
Example fuselage surface currents or “creeping wave” from array



## 2.1 Typical aircraft and mounting geometry

To properly address the question of fuselage attenuation, the typical commercial aircraft antenna configuration is explored. In 2022, the majority of the world's commercial aircraft (assumed  $> 45\%$ ) are either Boeing 737 or Airbus A320 models that have a fuselage diameter between 3.76 m to 3.95 m. This fuselage diameter may represent mid-sized aircraft. Other common commercial aircraft have larger fuselage diameters (e.g. Airbus A340 and Boeing 787) range in fuselage size from 5.64 m to 5.77 m. Common commercial aircraft that are smaller (e.g. Embraer E190) have fuselage diameters of approximately 3.0 m. Other antenna characteristics, aircraft types and mounting scenarios need to be considered in future additions to this Report. Moreover, additional modelling, such as a sensitivity analysis, showing that slightly different radii cylinders, or shapes that are slightly modified off of a purely cylindrical shape, would help verify that the cylindrical simplification of the fuselage in the simulation study has minimal impact on the results.

Due to the long and narrow nature of commercial aircraft fuselages, coupled with the need for high antenna gain, the aeronautical satellite connectivity community has settled on two main antenna configurations for commercial broadband connectivity: (i) upward looking electronically steered variable aperture (ES-VA) arrays and (ii) mechanically steered, fixed aperture (MS-FA)<sup>1</sup> arrays. Of these antenna configurations, the mechanically steered array has the widest adoption and is the focus of this analysis. Due to aerodynamic constraints, the antenna must have a narrow height above the aircraft fuselage but achieves high gain capabilities by increasing the width of the antenna array, giving the antenna a rectangular aperture configuration. The geometry of a typical mechanically steered antenna array is depicted in Figs 2 and 3.

---

<sup>1</sup> ETSI TR 103 233, Technical Report on antenna performance characterization for GSO mobile applications.

FIGURE 2  
Typical fuselage mounted antenna assembly

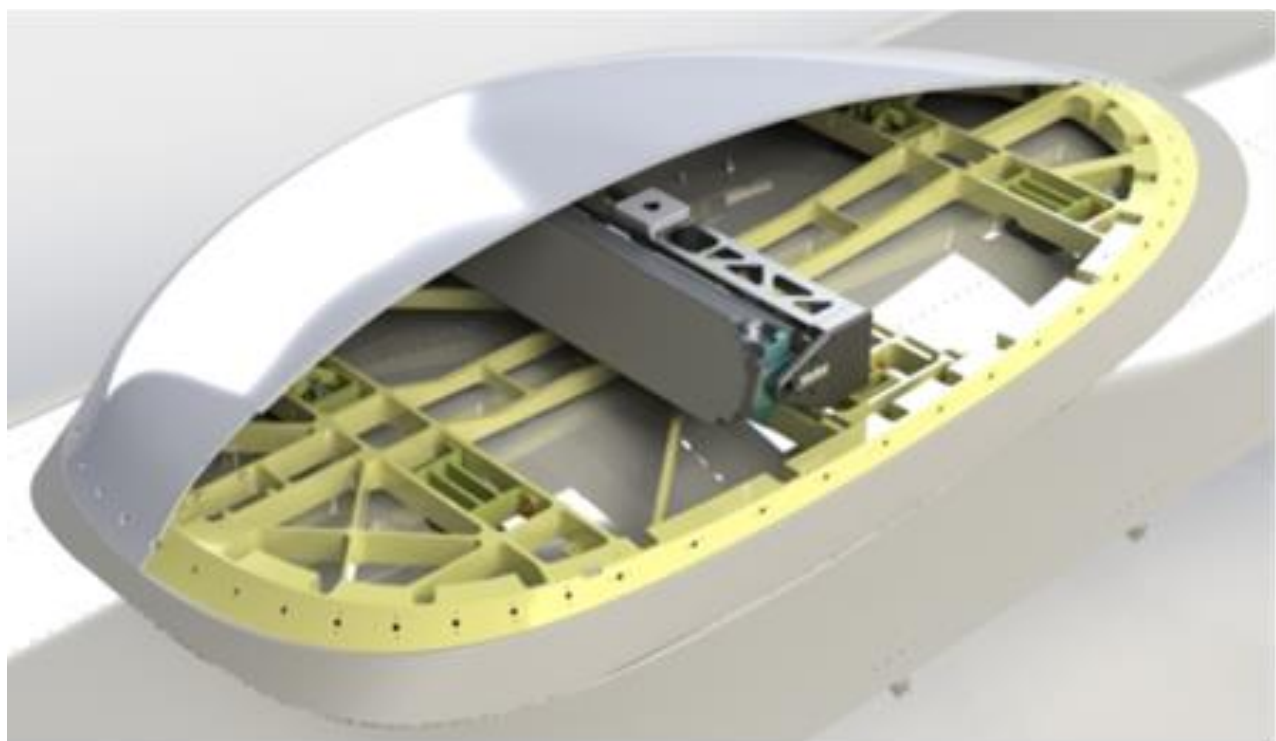
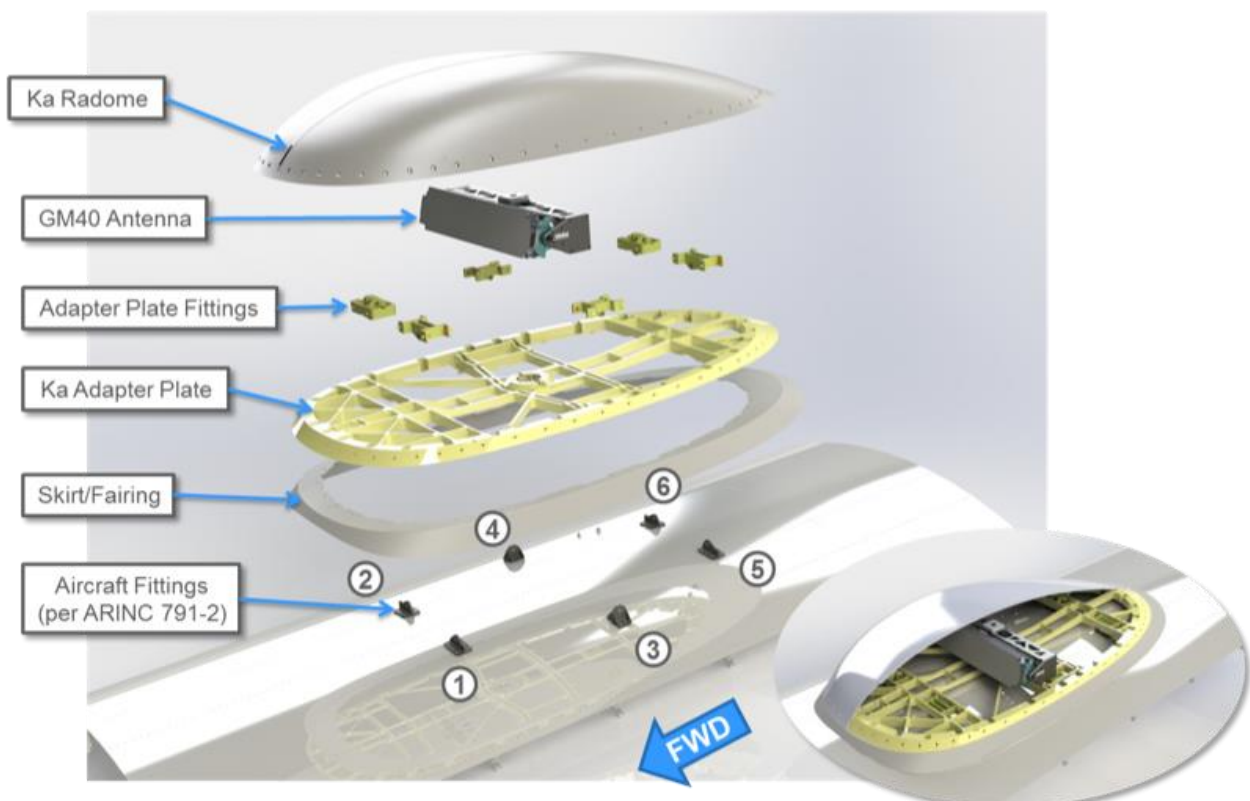


FIGURE 3  
Breakdown of the assembly by individual parts



## 2.2 Simulation details

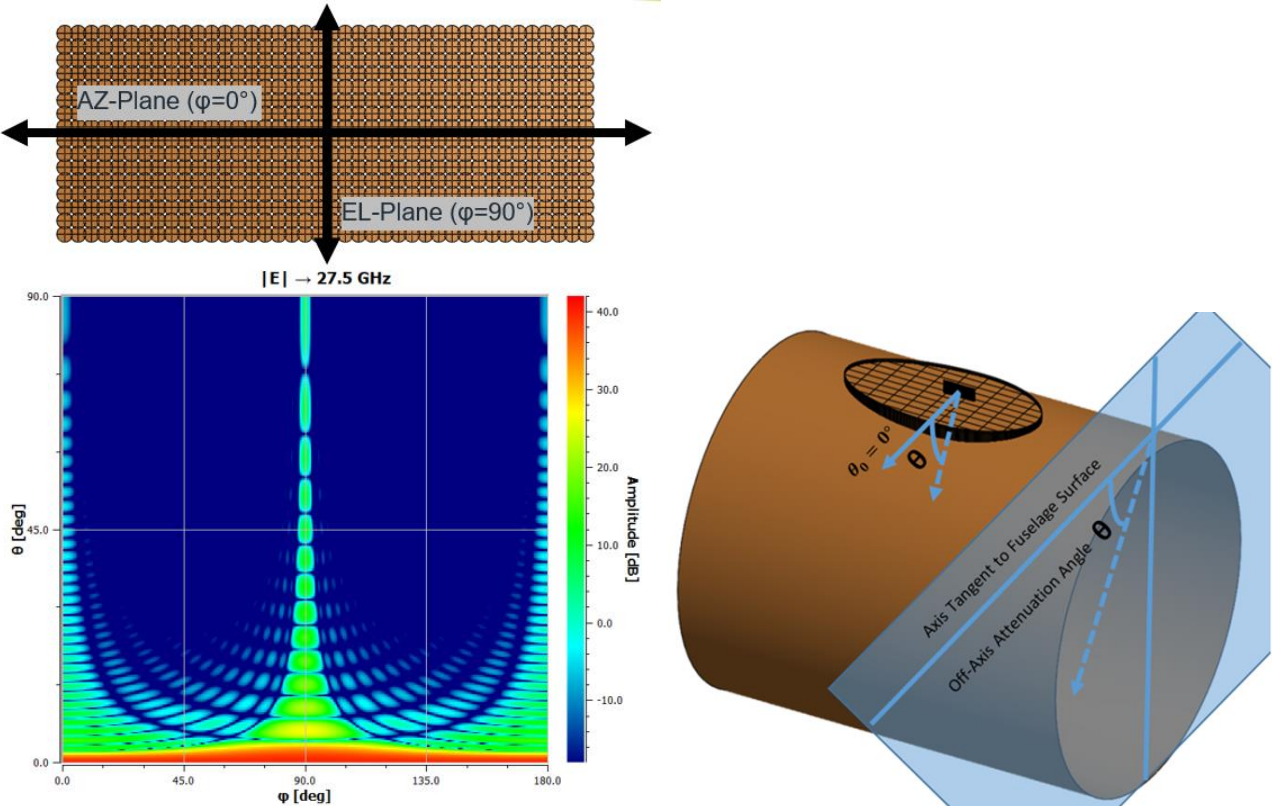
The following analysis includes a full-wave simulation using the method of moments (MOM) solver tool along with the multi-level fast multipole method (MLFMM) to simulate the electrically large environment in an accurate and efficient way. Specifically, this work uses the TICRA GRASP 10.6 tool. Any MOM solver could be similarly used. The simulations are performed using large computing nodes (needing roughly 500-1 000 GB of RAM to run the models) and 24-36 CPUs.

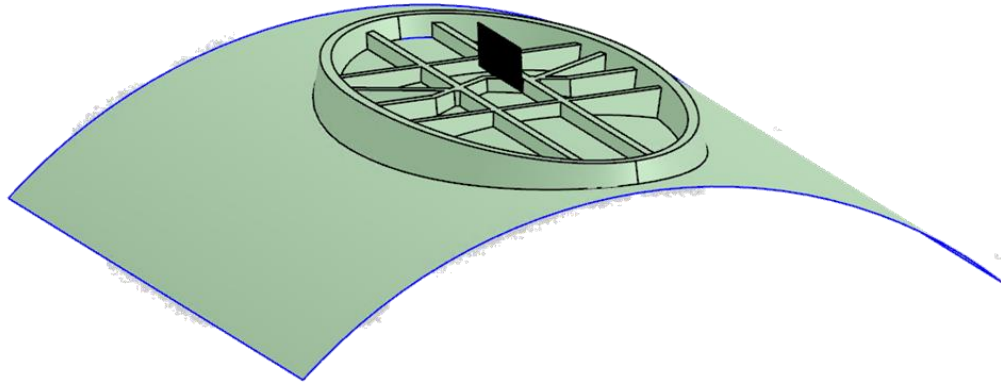
The electrical excitation source for the analysis (i.e. the antenna radiating above the fuselage) is a  $40 \times 16$  waveguide array modelled as individual circular apertures. (Note: the actual array is closer to  $80 \times 16$ , but this model produces similar results in the elevation plane (perpendicular to fuselage) as an approximation for accelerated computation. In the long dimension, or horizontal plane, the taper is a Taylor distribution and in the vertical plane the taper is uniform. Given these tapers, the beam is broadest and sidelobes are the highest in the elevation plane. The antenna model and free-space far field patterns are depicted in Fig. 4 (left). The antenna is located roughly 15 cm above the fuselage.

Two aircraft configurations are considered for this Report, namely, a 3.76 m and 5.77 m diameter cylinder, as described in the previous section, with the boundary condition as a perfect electric conductor (PEC) (see Fig. 4 (right)). The fairing is approximated as an ogival shape with draft and cross-bars as seen in Fig. 4 (bottom) with thickness, height, and shape approximately equal to that depicted in Figs 2 to 3 to reduce computational complexity and number of mesh faces. The off-axis angle orientation is also shown (see bottom right). The array is placed approximately 15.25 cm above the fuselage, and the fairing ring's height is set below the bottom element. The fairing ogive ring's thickness is approximately 3.8 cm with a slight draft angle. These parameters are based on actual fairing models.

FIGURE 4

Array-Only Model and Far Fields (left); Reference Geometry (right); Detailed Fairing Model (bottom)



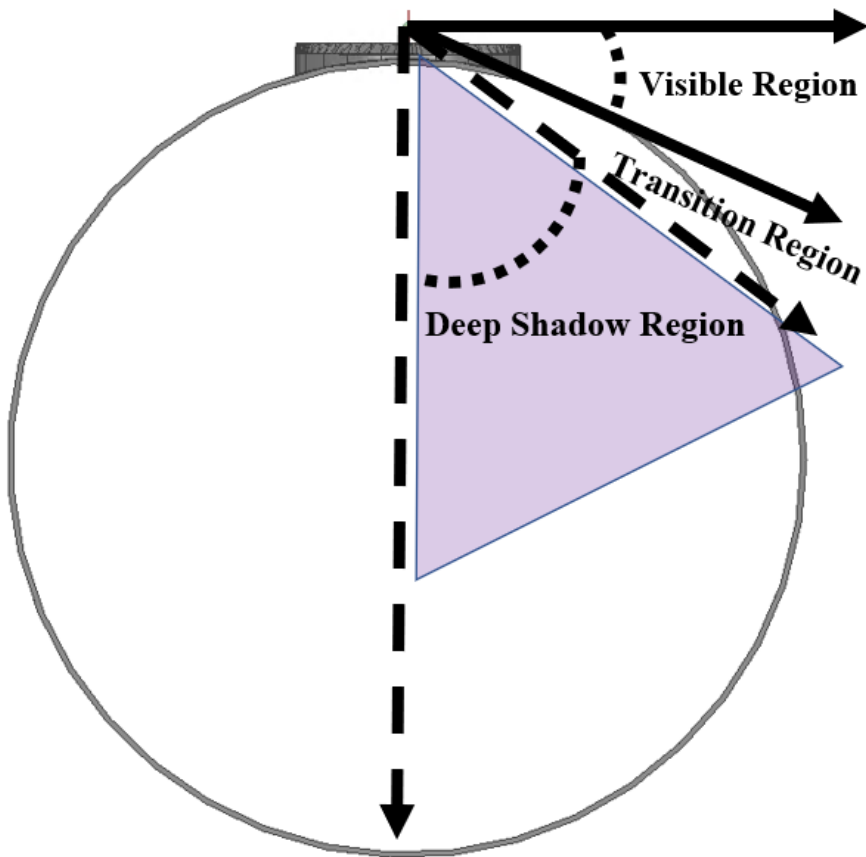


### 2.3 Solution regions

The following three regions are proposed as a framework for consideration of the fuselage attenuation analysis and solutions. The preliminary results section provide results from the visible and deep shadow region.

- Visible Region: This section is the line-of-sight region where, in the array and fuselage only case, a ray is traced from the phase centre on the array and is not blocked by the aircraft fuselage. This is the geometric non-blockage region.
  - For the 3.76 m diameter aircraft fuselage example, with a 15 cm antenna phase center above the cylinder, the visible region approximately corresponds to the angles of 0 degrees to 23 degrees.
  - For the 5.77 m diameter aircraft fuselage example, with a 15 cm antenna phase center above the cylinder, the visible region approximately corresponds to the angles of 0 degrees to 29 degrees.
- Deep Shadow Region: This section is the region where the excited surface currents, or "creeping waves", produce the far field environment independent of the antenna source.
  - For the 3.76 m diameter aircraft fuselage example, with a 15 cm phase centre above the cylinder, the deep shadow region approximately corresponds to the angles of 35 degrees to 90 degrees.
  - For the 5.77 m diameter aircraft fuselage example, with a 15 cm phase center above the cylinder, the deep shadow region approximately corresponds to the angles of 29 degrees to 90 degrees.
- Transition Region: This section is the region between the visible and deep shadow regions.
  - For the 3.76 m diameter aircraft fuselage example, with a 15 cm phase centre above the cylinder, the transition region approximately corresponds to the angles of 23 degrees to 35 degrees.
  - For the 5.77 m diameter aircraft fuselage example, with a 15 cm phase centre above the cylinder, the transition region approximately corresponds to the angles of 18 degrees to 29 degrees.

FIGURE 5  
Illustration of the solution regions under consideration



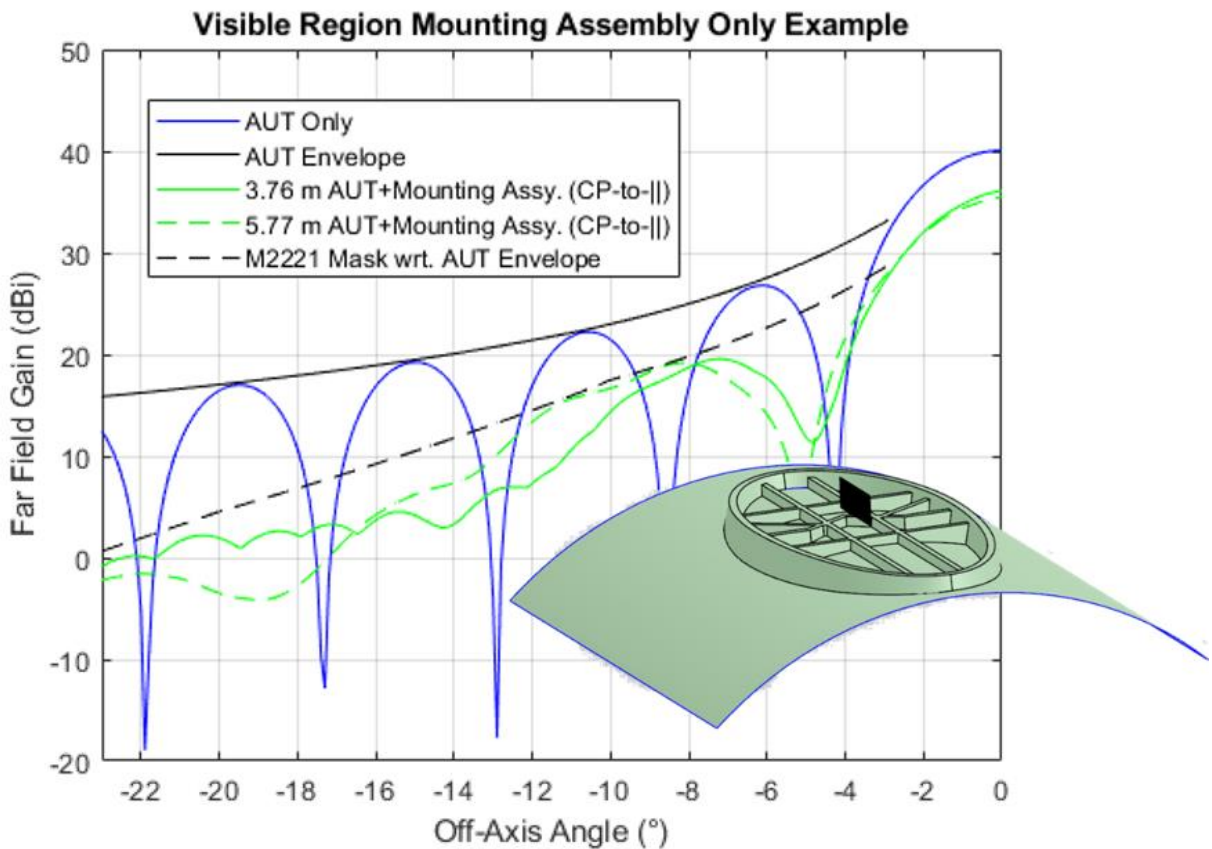
### 3 Simulation results

#### 3.1 Results: Visible region

To validate the Report ITU-R M.2221 mask in the visible region, a simulation is performed for the 3.76 m and 5.77 m adapter assemblies along with the upper portion of the fuselage corresponding to the visible region and some simple crossbar structures typical of the mounting assembly. This analysis will not yield results in the deep shadow or transition regions since the full fuselage is not in the model. Nonetheless, the model will yield results for the visible region. That is, the radome is not modelled but it will only increase the attenuation. The results are shown in Fig. 6 as well as the geometry of the analysis for the 3.76 m and 5.77 m cases. There is an assumed 1 dB radome loss in order to be consistent with the Report ITU-R M.2221 mask.

The results demonstrate that the Report ITU-R M.2221 result is almost exactly consistent for this region and no change is needed to the Report ITU-R M.2221 mask. The differences between the two fuselage sizes are minor and can be attributed to the differing local flatness or curvature of the fuselage (i.e. larger fuselage is more locally flat in the visible region).

FIGURE 6  
Visible Region Mounting Assembly



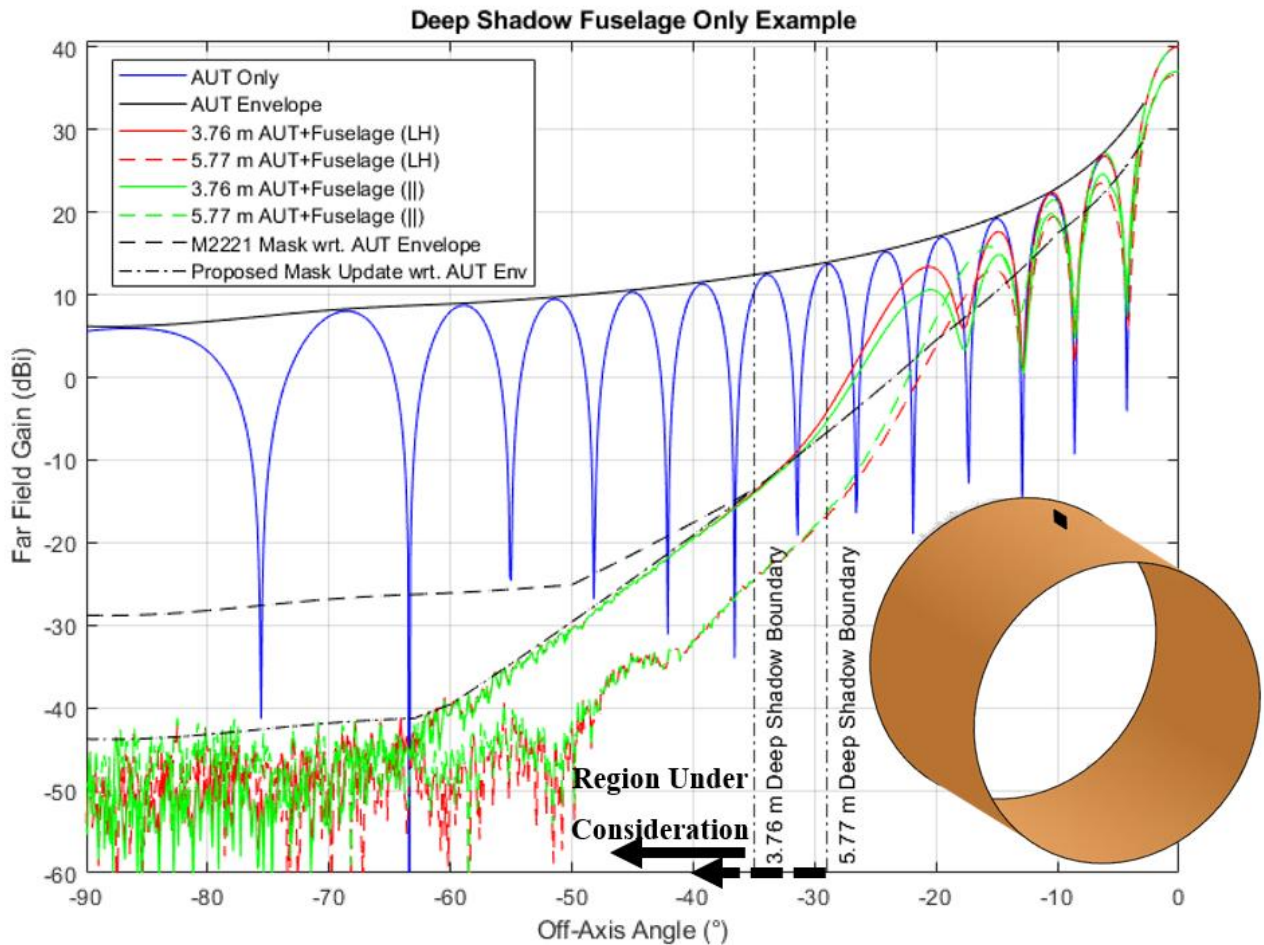
### 3.2 Results: Deep shadow region

To validate the Report ITU-R M.2221 mask in the deep shadow region, the aircraft fuselage-only scattering case is considered for both the 3.76 m and 5.77 m fuselage diameters. This analysis will not yield results in the visible or transition regions since there is no fairing or mounting adapter to scatter the transmissions. The analysis will yield results in the deep shadow region that are considered conservative. Adding the fairing and mounting adapter to the scatter will only increase the attenuation.

The results are shown in Fig. 7, where blue is the antenna (AUT) circular (CP) co-polarized (COPOL) far field in free space, black is the envelope for the free space AUT, red is the circular CP COPOL result including the aircraft fuselage, green is the worst-case linear result including the fuselage and the black dashed line is the Report ITU-R M.2221 mask offset by the AUT envelope.

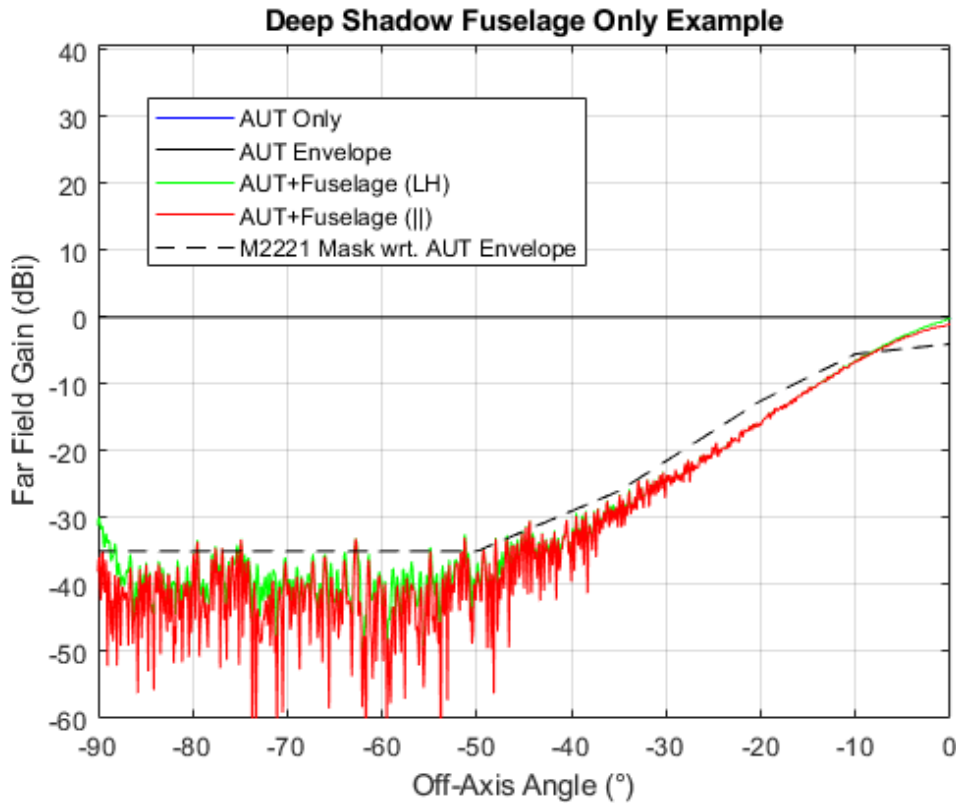
The results show that the Report ITU-R M.2221 result is consistent with the start of the region. The Report ITU-R M.2221 result flattens out the simulated result demonstrating that the aircraft fuselage linearly attenuates the fields. Therefore, the recommendation based on these results is that the Report ITU-R M.2221 mask should have the 50 degrees floor lowered further to account for the additional attenuation. This recommendation is plotted in Fig. 7 and is identified in the legend as “-.-“ mask title “proposed Mask Update wrt. AUT Env”.

FIGURE 7  
Deep shadow region fuselage



“Worst-case linear” represents the conservative case where attenuation is the weakest or  $\max(H, V)$  of the linear polarizations. Specifically, the “worst-case” represents the vertical “y” polarization or the perpendicular (  $\perp$  ) case with respect to the orientation of the fuselage providing the least attenuation (presented here). In the “best-case,” the polarization is horizontal “x” or the parallel (  $\parallel$  ) case with respect to the orientation of the fuselage providing the most attenuation (not depicted in this analysis but there is up to 10 dB of additional attenuation starting at the transition region). The formulations in this analysis are based on Ludwig’s third definition where the linear E co-polarization is on the “x” axis (horizontal/parallel) and the linear E cross-polarization is on the “y” axis (vertical/perpendicular) assuming  $\theta$  is zero for reference. Note: The worst-case circular polarization is always the co-polarized component because that is what the antenna radiates. While the analysis provides the “worst-case” circular and linear converge in the deep shadow region, the “best-case” (not shown) linear component provides even more attenuation.

FIGURE 8  
Simulated Ku OMNI source a-top fuselage



#### 4 Summary

Consideration of fuselage attenuation is important as this attenuation reduces emissions from the ESIM mounted on aircraft toward terrestrial stations on the Earth's surface. Full-wave simulations were conducted for a typical mechanically steered antenna array, operating within frequency range of 27.5-29.5 GHz, with two aircraft configurations, namely a 3.76 m and 5.77 m diameter cylinder. A similar analysis using measured data was previously conducted in Report ITU-R M.2221 under § 3.6.2.6.2 "Interference from aircraft earth stations to radio astronomy stations", specifically in Fig. 3.6-14. In this Report, fuselage attenuation results are provided for visible region, deep shadow region and transition region. The results demonstrate that, for visible region, the Report ITU-R M.2221 result is almost exactly consistent, and no change is needed to the Report ITU-R M.2221 mask. For deep shadow region, the results show that the Report ITU-R M.2221 result is consistent with the start of the region. The results show significant difference after 50 degrees off-axis angle with respect to the Report ITU-R M.2221 mask, demonstrating that the aircraft fuselage linearly attenuates the fields.

In addition, it should be noted that other antenna and aircraft combinations and mounting scenarios need to be considered in future additions to this Report. And as noted before, additional modelling, such as a sensitivity analysis, showing that slightly different radii cylinders, or shapes that are slightly modified off of a purely cylindrical shape, would help verify that the cylindrical simplification of the fuselage in the simulation study has minimal impact on the results.